ISSN 1330-3651(Print), ISSN 1848-6339 (Online)
UDC/UDK [536.7.08:620.193.2](498)

THERMODYNAMIC STUDY OF ATMOSPHERIC CORROSION SEASONAL KINETIC, BASED ON SUN PHOTOMETER DATA

Delia-Gabriela Calinoiu, Ioana Ionel, Mirjana Ševaljević, Milan Pavlović, Laszlo Makra, Ion Vetres, Gavrila Trif-Tordai

Original scientific paper

The atmospheric corrosion is a mechanical, technological, economic as well as an ecological problem, due to the enormous losses in corroded vessels material and machine material due to enhanced content of corroded material pollutants in environment. The results of the thermodynamic diagnostic study are given in this paper of the limited step in the water vapor corrosion kinetic based on the monitoring data for the seasonal water vapor pressure measured daily in Timisoara, by 2011, from March to December. Based on the seasonal values of the measured data, the seasonal diffusion rate constants the activation energies of the first chemical corrosion step are determined. The calculated seasonal water vapor chemical surface polarizations relative to the values of equilibrium entropies and also of the condensed water vapor on the solid surfaces are compared with the literature data of the possible products of chemical processes. The thermodynamic diagnostic study of the limited successive relaxation step in overall corrosion kinetic is carried out, based on the comparison of the molar water vapor couple relaxation work. The depolarization work is proportional to the depolarization rate constants of reactants and products activated successively in couple with water vapor concentrations depolarization energy, in the same time period: the electrochemical relaxation for the achievement of oxygen and hydrogen equilibrium in the seasonal activated corrosion cell, hydrogen depolarization energy and oxygen striping indicators standard potential. Data used to calculate the water vapor pressure in atmosphere are based on measurements accomplished by a sun photometer located at the Politechnica University of Timisoara, Romania (45,74 °N; 21,22 °E). The extraction of water vapor amount from sun photometer capacity relies on a measurement in the region of water vapor absorption at 940 nm. In order to apply the empirical models, the temperature, barometric pressure and humidity content have been taken from a weather station. One found that the experimental values of water vapor pressure, obtained using the sun photometer, are comparable with four other methods, and within, the experimental variations is characterized by a relative error of 2 %.

***Keywords**: chemical/electrochemical equilibrium, corrosion, hydrogen over potential, indicator of reversible and irreversible process, Sun photometer, water vapour, water vapour couple kinetic*

Termodinamičko proučavanje sezonske kinetike atmosferske korozije, na osnovu fotometrijskog određivanja tlaka vodene pare

Izvorni znanstveni članak

Zbog ogromnih gubitaka koji nastaju na strojarskim materijalima, atmosferska korozija predstavlja tehnološki, ekonomski, kao i ekološki problem zbog povećanja sadržaja onečišćenja u životnom okolišu. U ovom radu su prikazani rezultati termodinamičke dijagnostike ograničavajućeg stupnja ukupne kinetike korozije uslijed dodira čvrstih površina s vodenom parom, na osnovu podataka dobivenih svakodnevnim promatranjem tlaka vodene pare u Temišvaru 2011., od ožujka do prosinca. Na osnovu sezonskih vrijednosti izračunate su konstante difuzije vodene pare, nastale uslijed gradijenta koncentracije, kao i energije termokemijske aktivacije prvog stupnja korozije, na osnovu Ahrrenijusove jednadžbe. Izračunate relativne sezonske varijacije kemijske polarizacije vodene pare u odnosu na ukupnu promjenu entropije nastale i kondenzacijom na čvrstim površinama, uspoređene su s literaturnim vrijednostima za slobodne Gibbs-energije mogućih produkata relaksacijskih termokemijskih reakcija. Ograničavajući stupanj ukupnog procesa korozije, određen je usporedbom molarnog rada depolarizacije sukcesivnih elektrokemijskih relaksacijskih procesa. Depolarizacijski rad proporcionalan je konstanti brzine sezonski aktiviranih sukcesivnih relaksacijskih procesa u razdoblju koncentracijske depolarizacije vodene pare: elektrokemijske relaksacije kisika i vodika pri pretlaku depolarizacije vodika i standardnom potencijalu indikatora anodnog rastvaranja metala. Podaci rabljeni za izračunavanje tlaka vodene pare u atmosferi dobiveni su pomoću fotometra iz meteorološke stanice na "Politihnici" Sveučilišta u Temišvaru, Rumunjska (45,74 °N; 21,22 °E). Mjerenja su provedena u području valnih duljina 940 nm, uporabom empirijskih modela i podataka o temperaturi, barometarskom tlaku i vlažnosti zraka, a suglasne su s rezultatima 4 različite metode s varijacijama do 2 %.

***Ključne riječi**: indikator anodnog rastvaranja metala, kemijska/elektrokemijska ravnoteža, kinetika udruženih reakcija vodene pare, korozija, pretlak vodika, "Sun" fotometar, vodena para*

1 Introduction

Earth's atmosphere contains roughly 78,08 % nitrogen, 20,95 % oxygen, 1,247 % water vapor (a variable amount), 0,93 % argon, 0,038 % carbon dioxide and other gases. This value was determined by National Center for Atmospheric Research (http://ncar.ucar.edu/). This water vapor makes up less than 0,001 % of all the water on the Earth and this is important to our climate.

Aerosols play important role in global climate change by increasing backscattered solar radiation and by absorbing solar and long wave radiation and also, by altering cloud properties.

Sun photometry has the capability to describe characteristic features of different air masses and the aerosol sources that affect the climate. Aerosol optical depth and size distributions can be derived remotely through solar direct beam measurements at a range of wavelengths and zenith angles [1, 2, 3]. A sun photometer is an optical instrument for the measurement of the spectral solar radiation. The spectral resolution depends on the number of channels. The range of wavelength is between 340 ÷ 1640 nm. The 940 nm channel is used for column water abundance determination.

The AErosol RObotic NETwork [4] is a global network of sun photometers. In this network exist over 700 instruments, 5 of them being in Romania (Holben et al., 1998). The network hardware consists of identical automatic sun–sky scanning spectral radiometers owned by national agencies and universities. AERONET provides not only spectral aerosol optical depth, but also derived aerosol properties, such as, single-scattering, asymmetry parameter, phase function, and size distributions of aerosol particles at a given location. In Timisoara other data regarding air quality is performed by

Polytechnic University of Timisoara mobile laboratory [5, 6, 7, 8] and LIDAR system [9].

This paper presents the results of continuous measurements of aerosol optical properties from whence is extracted the amount of water vapor over Timisoara for almost one year. The amount of water in the atmosphere is extracted from values recorded by the weather station, using several methods. The measurements taken from weather station and used in this paper include temperature, barometric pressure and humidity. This analysis is very important, because water vapor represent the most potent greenhouse gas.

Water vapor condensation on metal surface can cause electrochemical – atmospheric corrosion (as well as in humid soil and electrolyte solution, hydrogen or /and oxygen i.e., stationary mixed corrosion polarization on homogeneous or pitted and trans-crystal and inter-crystal alloy corrosion.

The complex corrosion process overall kinetic, in presence of chemical reactant (diffusion, electrochemical heterogeneous reaction and desorption of indicator of stationary cathode and anode mixed polarization), affects considerably the seasonal water vapour pressure. The seasonal equilibrium of water vapour influences chemical potential in the different complex materials of solid and liquid phases (which contain many mineral and organic substances Fe, Mn, Cr, Pb, Cd, nitrogen, sulphur, halogen phosphorus, carbon, etc.)

An important contribution [12, 13] to the investigation of corrosion kinetics indicates the greatest rate constant for coal activation as anode in the presence of the strongest oxidizing agent, namely the redox couple Mn^{7+}/Mn^{2+} is found. The rate constants in the presence of other oxidants decrease in the following order: $Cr^{6+}/Cr^{2+} > V^{5+}/V^{4+} > Fe^{3+}/Fe^{2+}$. The greatest rate constant, and thus the most efficient gasification was effected in the presence of sulphuric acid as supporting electrolyte. This fact points out to the influence of the nature of the solvated complex ion, which is involved in the step of coal surface activation as local anode. The electrochemical coal gasification proceeds firstly via chemical reaction with the oxidant, and the least activation energy depending on contact surface between coal and oxidant ion. This reaction takes place without current passing. Chemical oxidized solid coal, during the second step of the condensation centre for water vapour, reacts with liquid water, giving rise to $CO_{2(g)}$ and hydrogen ions, in galvanic cells, when corrosion current is successively switched on. Hydrogen ions are reduced on Fe cathode and Fe^{2+} ions are re-oxidized on anode to Fe^{3+}, or in presence of other corrosion agents then iron (Mn, Cr, V) which control activation energy of corrosion process [13].

The paper [14] applies the thermodynamic diagnostic study of electron density in gas bubbles in aerated refinery waste water. The analysis results indicate to evolved hydrogen polarization about 0,41 V enabling electrochemical equilibrium with atmospheric oxygen and saturated water vapour in air bubbles .

The objective of this paper is thermodynamic study of atmospheric corrosion seasonal kinetic based on the sun photometer data of the water vapour pressure. The obtained results could enable to choose optimized corrosion protection and water vapour striping processes in catalytic metals deposition, depending on the seasonal conditions.

2 Experimental procedure

The sun photometer and weather station is located on the roof of the Mechanical Engineering Faculty of Polytechnic University of Timisoara (Fig. 2), with coordinates: 45,74 °N; 21,22 °E. The sun photometer from Timisoara is connected at AERONET site (http://aeronet.gsfc.nasa.gov), ranking #645. The sun photometer major components are an optical head, an electronic box and a robot [10].

Figure 1 Sun photometer and weather station located at Polytechnic University of Timisoara

The optical head has two channel systems: the sun collimator and the sky collimator. The sun tracking is equipped with a 4-quadrant detector. The electronic box contains two microprocessors for real time operation for data acquisition and motion control. In automatic mode, a ‘wet sensor′ detects precipitation and forces the instrument to park and to protect the optics. The robot is moved by step-by-step motors in two directions: in the zenith and azimuth planes.

The sun photometer accomplishes two basic measurements, either direct sun or sky, both within several programmed sequences. The direct sun measurements are made in nine spectral bands (340, 380, 440, 500, 670, 870, 940, 1020 and 1640 nm) requiring approximately 10 seconds. The 940 nm channel is used for column water abundance determination.

Sky measurements from March to December 2011 in Timisoara are performed, at 440 nm, 670 nm, 870 nm, and 1020 nm. Two basic sky observation sequences are recorded: the "almucantar" and the "principal" plane.

Sun photometer measures the spectral extinction of the direct solar radiation. This is expressed in the Beer-Lambert-Bouguer law:

$$V(\lambda) = V_0(\lambda)\left(\frac{d_0}{d}\right)^2 \exp(-\tau \cdot m), \quad (1)$$

where:
V is the digital voltage, V
V_0 − extraterrestrial voltage, V
λ − wavelength, nm
m − optical air mass (airmass factor), −
d_0 − the average Earth - Sun distance, expressed in astronomical units (ua)
d − the Earth - Sun distance on the day of observation, expressed in astronomical units (ua)
τ_t − total atmospheric optical thickness.

The air mass is calculated as function of the solar zenith angle. Absorption by water vapour is restricted to narrow spectral bands. The extraction of water vapour amount from sun photometer measurements generally relies on a measurement in the region of water vapour absorption at 940 nm. The aerosol effect is removed by extrapolating the value based on an adjacent band outside the absorption or, by interpolation between two adjacent bands. Equation 1 is not valid since exponential attenuation applies strictly to monochromatic radiation and is invalid across the broad region of water vapour absorption.

Transmission in the water vapour band (T_w) can be modelled [10] as:

$$T_w = \exp(-am^b W^b), \quad (2)$$

T_w − transmission in the water vapour
W − vertical column abundance
a, b − constants depend on the wavelength position, width and shape of the sun photometer filter function, and the atmospheric conditions.

3 Results and discussions

The average amount of water vapour in the period studied has a value of 1,405 cm, with an error of 1,0039 %. The variation of water vapour calculation with different methods, depending on the Julian day in Timisoara, between March - December by 2011, is presented in Fig. 3. Values obtained by the method used to calculate amount of water vapour from the specific 970 nm wavelength of sun photometer are between the four methods of calculation, based on data from the weather station [10, 11].

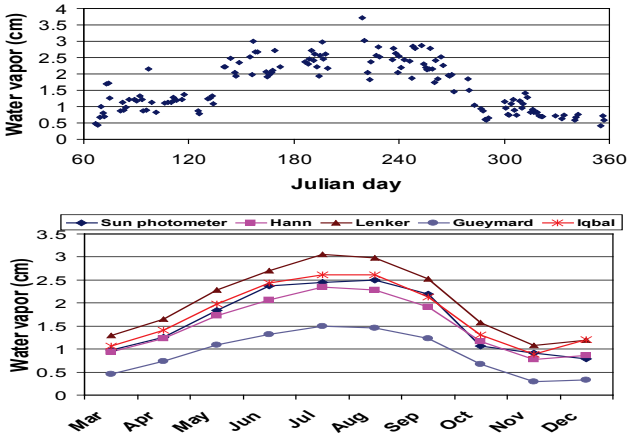

Figure 3 Water vapour measured with the sun photometer from March (67 Julian day) to December (356 Julian day) by 2011, in Timisoara, with about 15 ÷ 30 data measured each day, from 7 ÷ 19 GMT [10]

Table 1 Experimental data for water vapour pressure and temperature and the Table data for the saturated water vapour pressure and molar gas pressure

Month	Water vapour exp. pressure h_w / cm	Rel. error $\pm\Delta h/h$ / %	Temper. ϑ / °C	Wat. vap. pressure p / Pa	Sat. water vapour pressure p^* / Pa	Molar gas pressure p_G / Pa
March	0,979	1,488	6,336	1293	893	2324
April	1,251	1,748	12,653	1668	1270	2376
May	1,844	1,121	16,411	2158	2447	2407
June	2,368	0,809	20,959	3157	2384	2445
July	2,453	0,739	22,291	3270	2406	2456
August	2,493	0,585	22,932	3324	2417	2462
September	2,192	0,572	20,599	2292	2378	2442
October	1,066	0,936	10,548	1421	1249	2359
November	0,915	0,848	2,933	1220	634	2295
December	0,786	1,935	3,161	1048	636	2297

In this paper the water vapour pressure ratio with molar gas pressure at equal seasonal air temperatures is compared with real measured and equilibrium Table data (Fig. 1).

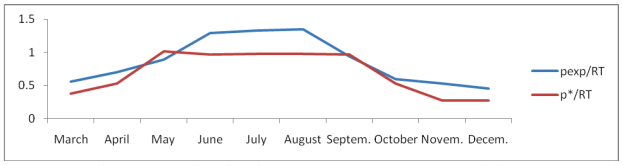

Figure 2 The seasonal ratios between water vapour partial pressure and molar gas pressure RT, for water vapour measured data in Timisoara by 2011, p_{exp} and for saturated water vapour pressure Table data, p^*

The results in Fig. 2 point to the equilibrium between measured and saturated water vapour pressure and molar gas pressure, $p_{exp}/RT = p^*/RT = 1$ in May and September.

Atmospheric corrosion seasonal kinetic study is based on the dependence of water vapour content on the time, calculated from the beginning point, 1st January when equilibrium of three water phases is achieved at $T_0 = 273$ K. The fitted experimental data (with correlation coefficients, R^2 = 0,78 in autumn, and in spring and summer with the R^2 = 0,95 ÷ 0,98), confirm water vapour diffusion mass transport activated with surface reactions corresponds to the first order kinetic and makes possible determination of the seasonal water vapour diffusion rate constants:

$$\ln h = k_d \cdot \tau + \ln h_0, \quad (3)$$

$$\tan\alpha = k_d. \quad (4)$$

The obtained diagrams indicate that experimental data fit the first order reaction kinetic with strong correlation coefficients (Tab. 2).

Table 2 The first order kinetic law for experimental determination of water vapour seasonal values diffusion rate constants

Month	Day in year	Water vapour first order kinetic law $\ln h = -k_d \tau + \ln h_0$	Correl. coeff. R^2	Diffusion rate con. k_d /day^{-1}
March	67	$0{,}0104\tau - 0{,}7399$	0,999	0,0104
April	97	$0{,}0104\tau - 0{,}7399$	0,99	0,0104
May	128	$0{,}0104\tau - 0{,}7399$ $0{,}0059\tau - 0{,}1197$	0,99 0,95	0,0104 0,0059
June	158	$0{,}0059\tau - 0{,}1197$	0,95	0,0059
July	189	$0{,}0059\tau - 0{,}1197$ $-0{,}0032\tau + 1{,}5872$	0,95 0,95	0,0059 −0,0032
August	219	$-0{,}0032\tau + 1{,}5872$	0,95	−0,0032
September	248	$-0{,}0032\tau + 1{,}5872$ $-0{,}0087\tau + 2{,}7343$	0,95 0,79	−0,0032 −0,0087
October	279	$-0{,}0087\tau + 2{,}7343$	0,79	−0,0087
November	310	$-0{,}0087\tau + 2{,}7343$	0,79	−0,0087
December	356	$-0{,}0087\tau + 2{,}7343$	0,79	−0,0087

Activation energy of water vapour phase and chemical transformation on active centres, which control water vapour diffusion rate constants are determined on the basis of slope of Arrhenius equation, $\tan\alpha$ according to Eq. (6):

$$\ln k = \frac{E_a}{RT} + \ln k_0, \tag{5}$$

where:

$$E_a = R \cdot \tan\alpha. \tag{6}$$

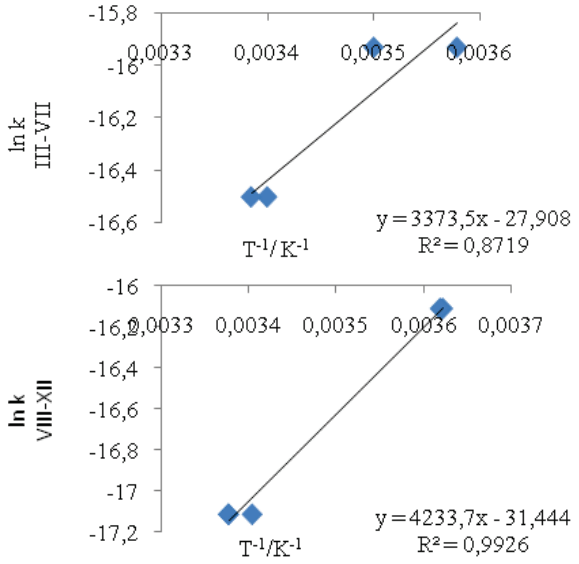

Figure 4 The experimental data fitted Arrhenius equation (5), for determination of water vapour couple activation energy

The activation energy of water vapour pressure is calculated:

(a) for the seasons from March to July:

$E_{a(III\text{-}VII)} = -28{,}047$ kJ/mol,

when it corresponds to the free energy of possible cathode corrosion agent:

$E_{a(III\text{-}VII)} = \Delta G^{\theta}(NH_{3aq}) - RT_{con.cen.}/2 \cong (-26{,}6 - 348R/2)$ kJ/mol.

(b) for the seasons from August to December:

$E_{a(VIII\text{-}XII)} = -35{,}2$ kJ/mol

Then it corresponds to the free energy of the possible corrosion agents:

$$E_{a(VIII\text{-}XII)} = -((\Delta G^{\theta}(Fe/Fe^{2+}) - \Delta G^{\theta}(OH)_{aq}))$$
$$E_{a(VIII\text{-}XII)} = -\Delta G^{\theta}(OH)_g$$
$$E_{a(VIII\text{-}XII)} = -\Delta G(O_2^-)_{aq} + 3/2RT_0 \text{ kJ}\cdot\text{mol}^{-1}$$

The aim of this paper, the thermodynamic study of atmospheric corrosion of seasonal activated condensation active centres, enables the determination of condensed liquid water free energy according to Gibbs equation (7).

$$\Delta G_w^{\theta} = \Delta H_{w,v,exp.}^{\theta} - T\Sigma\Delta_{tot}S^{\theta}, \tag{7}$$

where:

$$T\Sigma\Delta_{tot}S^{\theta} = T\Delta_{g,l}S^{\theta} - \Delta_{cond}H^{\theta *}, \tag{8}$$

$$\Delta_{cond}H^{\theta *} = -44{,}1 \text{ kJ/mol},$$

$$\Delta_{g,l}S^{\theta} = \Delta S_{w(L)}^{\theta} - \Delta S_{w\cdot v(G)}^{\theta},$$
$$\Delta_{g,l}S^{\theta} = 69{,}9 - 189 = -118{,}8 \text{ J/(mol}\cdot\text{K)}. \tag{9}$$

The experimental data for seasonal water vapour pressure and air temperature fit Clausius-Clapeyron Eq. (10), (the linear dependences of logarithm of measured real water vapour pressure in atmosphere on the reciprocal value of absolute temperature, T^{-1}) and enable the diagnostic of real water vapour enthalpy, $\Delta H^{\theta}_{w,v,exp.}$ according to Eq. (11).

Real water vapour molar enthalpy is calculated on the basis of the slope $\tan\alpha$, according to Eq. (11).

$$\ln h = \frac{\Delta H_{w,yv,exp.}^{\theta}}{RT} + \ln h_0, \tag{10}$$

$$\Delta H^{\theta}{}_{w,v,exp.} = R \cdot \tan\alpha. \tag{11}$$

The stationary polarization of corroded metal exposed to the water vapour pressure controls diffusion kinetic.

The carried out thermodynamic diagnostic study (Tab. 5) indicates the water vapour diffusion molar work can be calculated according to Eq. (12).

$$F\eta_d = RTk_d \cdot \tau. \tag{12}$$

The annual average activation energy, equal to that of reversible reduced oxygen to superoxide anion, confirms that water vapour molecules achieve thermal energy, $e\varphi$=3RT/2 in May and September (Fig. 2), and the average activation energy in couple with free energy of superoxide anion is acc. to Eq. (13):

$$E_{a,ann} = \frac{E_{a(III-VII)} + E_{a(VII-XII)}}{2}, \quad (13)$$

$$E_{a,ann} = -(\Delta G^{\theta}(O_2^-)_{aq} \pm 3/2RT_b)\ \text{kJ/mol},$$

were:

$$(\Delta G^{\theta}(O_2^-)_{aq} = 31{,}84\ \text{kJ/mol}.$$

Galvanic cell with free energy, equal to the corrosion work, calculated acc. to Eq. (14), activates irreversible relaxation processes with free energy equal to:

- mixed quasi-reversible polarization of indicator of hydrogen and oxygen corrosion type, acc. to Eq. (15)
- mixed stationary polarization of depolarized hydrogen, as well as water vapour diffusion over potential, through double water film, acc. to Eq. (16):

$$\Delta G^{\theta}_{corr} = F\Delta\varphi = \Delta G^{\theta}(O_2^-)_{aq} - \Delta G^{\theta}_{w}, \quad (14)$$

Table 3 The Clausius-Clapeyron's equations fitted seasonal experimental data, Eq. (10), the correlation coefficients, R^2, and the calculated: water vapour enthalpy, $\Delta H^{\theta}_{w,exp}$, Eq. (11), equilibrium exchanged water vapour entropy heat, $T\Sigma\Delta S^{\theta}$, Eq. (8) and water vapour free energy, ΔG^{θ}_{w}, Eq. (7)

Month	Clausius-Clapeyron Eqs $\ln w = \Delta H^{\theta}_{ev}/RT + \ln w_0$	Correlation coefficients, R^2	Experimental determined water vapor enthalpy $\Delta H^{\theta}_{w,exp}$ / kJ/mol	Equilibrium released water vapour enthalpy on cond. cen. $T\Sigma\Delta_{tot}S^{\theta}$ / kJ/mol	Calculated water vapour free energy ΔG^{θ}_{w} / kJ/mol
March	$y=-4864{,}1x+17{,}3456$	0,92	40,44	10,9	29,54
April	$y=-4864{,}1x+17{,}3456$	0,92	40,44	10,15	30,29
May	$y=-4864{,}1x+17{,}3456$ $y=-5106{,}7x+18{,}243$	0,92 0,99	40,44 42,46	10,15 9,16	30,74 33,30
June	$y=-5106{,}7x+18{,}243$	0,99	42,46	9,16	33,30
July	$y=-5106{,}7x+18{,}243$ $y=-5836{,}2x+20{,}668$	0,99 0,72	42,46 48,52	9,16 9,00	33,46 39,52
August	$y=-5836{,}2x+20{,}668$	0,72	48,52	8,93	39,60
September	$y=-5836{,}2x+20{,}668$ $y=-4274x+15{,}273$	0,72 0,93	48,52 35,53	9,20 9,20	39,32 26,33
October	$y=-4274x+15{,}273$	0,93	35,53	10,4	26,14
November	$y=-4274x+15{,}273$	0,93	35,53	11,3	24,23
December	$y=-4274x+15{,}273$	0,93	35,53	11,27	24,26

Table 4 The water vapour chemical corrosion agents' free energies of ΔG^{θ}_{w}, determined on the basis of equal free energy of the couple components using the table data [15], within deviation up to 3 %

Month	ΔG^{θ}_{w} / kJ/mol	The identified resonance free energies of the possible water vapour polarisations [15], ΔG^{θ}_{w} / kJ/mol	Formula of the possible corrosion agents [15]
March	29,54	(13,38+15,6) / −27,2 −30,5	$((PH_3(g) + Cu(NH_3)^{2+}aq) / ((Sn/Sn^{2+}aq)\,(Cu(NH_3)_2{}^{2+}_{aq}$
April	30,29	31,283 / −30,5	$Fe_2N_{(s)} / (Cu(NH_3)_2{}^{2+}_{aq}$
May	32,02	16,3 31,84 / −31,8 −31,162 −16,5	$O_{2diss}\,(O_{2(g)}+e = O_2{}^-_{aq}) / S_2Cl_2\,(Fe_3W_2)\,NH_{3(g)}$
June	33,30	16,3 34,22 / −33,56 −16,5	$O_{2diss}\,(OH_{(g)}) / S_2Cl_{2(g}\,NH_{3(g)}$
July	36,49	36 36,99 / -37	$H_2N_2O_{2aq}\,C_3H_7SSC_3H_{7(g)} / NO_2^-$
August	39,60	(50,3−(13,38+2,3)= 39,22 /−12,925 −26,6 =−39,5	$(Cu_{aq}{}^{+} - (PH_3(g) - RT_0) / (Fe/Fe^{3+}/3H^+/3H) - RT) - (NH_3)_{aq})$
September	32,82	16,3 (31,84) (32,221)/(−31,8) (−31,162) −16,5	$(O_2{}^-_{aq} = O_{2(g)}+e)\,Fe_4N_{(s)} / S_2Cl_2\,(Fe_3W_2)\,NH_{3(g)}$
October	26,14	26,1 26,65 / −27,87	$Fe_3C_{(s)}\,(CH_3SC_4H_{(g)}) / H_2S_{aq}$
November	24,23	24,1 24,32 23,4 / −23,3 −24,3	$\eta(O_2)/Fe\ P_4\ NH_2OH / (Fe_{1,111}\,Te_{(s)}\,Pb/Pb^{2+}$
December	24,26	24,1 24,32 23,4 / −23,3 −24,3	$\eta(O_2)/Fe\ P_4\ NH_2OH / (Fe_{1,111}\,Te_{(s)}\,Pb/Pb^{2+}$

Table 5 Thermodynamic diagnostics results for: water vapour molar activation energy, Eq. (6), Polarization of corrosion cell, Eq. (14), Mixed corrosion indicator standard potential, Eq. (15), Water vapour diffusion over potential, Eq. (12), Hydrogen over potential, Eq. (16) and molar gas pressure $p^{\theta}* = RT_{w\cdot v} = RT$

Month	Activation energy E_a / kJ/mol	Polariz.of corrossion cell ΔG^{θ}_{cor} / kJ/mol	Mixed cor. Ind. st. pot. FE^{θ}_{ind} / kJ/mol	Water vapour diff. overpot. $F\eta_d$ / kJ/mol	Hydrogen over potential $F\eta_{H2}$ / kJ/mol	Molar gas pressure $p^{\theta}* = RT$ / kJ/mol
March	−28,05	2,30	2,98	1,62	−2,77	2,32
April	−28,05	1,55	0,80	2,30	−3,08	2,41
May	−28,05	1,10	−3,50	3,08	−3,05	2,41
June	−28,05	−1,46	−5,20	2,28	−1,55	2,41
July	−28,05	−1,62	−9,30	2,74	6,32	2,41
August	−35,20	−7,76	−12,34	−3,18	7,31	2,51
September	−35,20	5,51	12,96	−2,75	3,24	2,41
October	−35,20	5,70	13,51	−2,11	−0,74	2,32
November	−35,20	7,61	17,50	−2,28	−1,53	2,32
December	−35,20	7,58	22,27	−7,11	3,32	2,32

$$\Delta G^{\theta}_{\text{corr}} = \frac{F \cdot E^{\theta}_{\text{ind}} + F \cdot \eta_{\text{dif,ind}}}{2},$$

where: (15)

$$F \cdot E^{\theta}_{\text{ind}} = 2\Delta G^{\theta}_{\text{corr}} - F \cdot \Delta\eta_{\text{d}},$$

$$\Delta G^{\theta}_{\text{corr}} = 2F \cdot \eta_{H2} + 2F \cdot \Delta\eta_{\text{d}},$$

where: (16)

$$F\eta_{H2} = -\frac{2F \cdot \Delta\eta_{\text{d}} + \Delta G^{\theta}_{\text{corr}}}{2}.$$

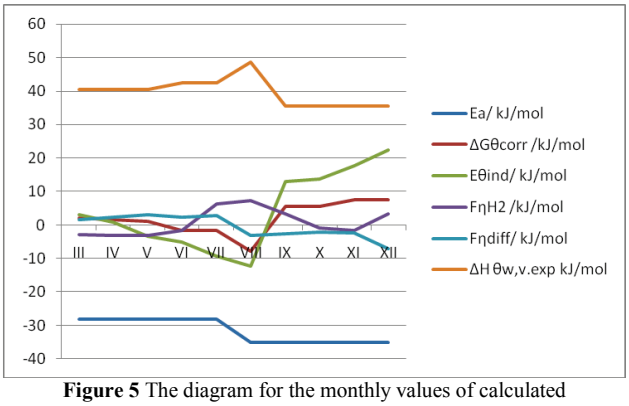

Figure 5 The diagram for the monthly values of calculated thermodynamic parameters

According to the monthly values of calculated thermodynamic parameters (Fig. 5) the couple process minimal free energy ($\Sigma\Delta G$=0) i.e., the thermal relaxation of water vapour pressure p_{exp}=p*=RT (Fig. 2) enables following two aspects:

- in May, the equal hydrogen over potential with mixed corrosion indicators standard potential,
- in September, the polarization of corrosion cell equal to hydrogen over potential and mixed corrosion indicators standard potential.

The diagnosed water vapour enthalpy in seasons from March to September (Tab. 3) indicates fast relaxation process of hydrated electron polarized in the beginning of electron titration at $\varphi_{\text{c.begin}} = -\Delta H^{\theta}_{\text{w,exp}}/F = -0{,}419$ V (March), −0,44 (June) and −0,502 V (August).

All metals with the stationary polarizations more negative than −0,414 V become thermodynamically instable and are chemically dissolved with hydrogen evolution.

The complex atmospheric corrosion seasonal kinetic control polarization work calculated as the sum of activation energy and water vapour enthalpy according to the Eq. (17):

$$F\varphi_{\text{cath0}} = E_{\text{a}} + \Delta_{\text{rel}} H^{\theta}_{\text{w,v,exp}}. \quad (17)$$

The combining with the measured data for activation energy (Tab. 5) and water vapor enthalpy (Tab. 3) give the next results from March to August:

$F\varphi_{\text{H2,III-V}} = T\Delta S^{\theta}(H_2O)_{\text{L}} - \Delta G^{\theta}(O_2^-)_{\text{aq}} = \Delta_{\text{diss}} H^{\theta}(O_2)$
$F\varphi_{\text{H2,VI,VII}} = T\Delta S^{\theta}(H_2O)_{\text{L}} - \Delta G^{\theta}(O_2^-)_{\text{aq}} + RT$
$F\varphi_{\text{H2,VIII}} = T\Delta S^{\theta}(H_2O)_{\text{L;}}$

The evolved hydrogen polarization from March to May controls oxygen spontaneous dissolution enthalpy equal to liquid water entropy in couple with superoxide anion free energy. In June and July one noticed the raise of the oxygen spontaneous dissolution enthalpy for the vibration energy and in August the drop to the liquid water entropy heat.

These results agree with previously obtained data in the examination of water entropy driven relaxation processes of dissolved oxygen in refinery waste water [16].

The calculated results (Tab. 5), indicate to the seasonal hydrogen over potentials, controlled from March to August with the indicator reversible titration , quasi-reversible water vapor diffusion and corrosion cell couple up to achieving hydrogen over potential closely corresponding to iron ($\eta(H_2/Fe)$ =7,31/96,5 ≈ 0,08 V, in August):

$F\eta_{\text{H2,III}} = FE^{\theta}_{\text{in,III}} = -2{,}77$ kJ/mol
$F\eta_{\text{H2,IV}} = -(FE^{\theta}_{\text{in}} + RT)_{\text{IV}} = -3{,}08$ kJ/mol
$F\eta_{\text{H2,V}} = FE^{\theta}_{\text{ind}} = -F\eta_{\text{d,V}} = -3{,}05$ kJ/mol, in May
$F\eta_{\text{H2,VI}} = \Delta G_{\text{corr VI}} = (2/3)F\eta_{\text{d}} = -1{,}5$ kJ/mol
$F\eta_{\text{H2,VII}} = -F(\eta_{\text{d}} + E^{\theta}_{\text{in}})_{\text{VII}} = 6{,}3$ kJ/mol
$F\eta_{\text{H2,VIII}} = -\Delta G^{\theta}_{\text{corr,VIII}} = 7{,}31$ kJ/mol

According to the Eq. (18), the couple between activation energy (Tab. 5) and water vapour enthalpy (Tab. 3) by the end of September up to December indicate to adsorbed hydrogen depolarization processes:

$$F\varphi_{\text{cath0}} = E_{\text{a}} + \Delta H^{\theta}_{\text{w,v,exp}} = 0. \quad (18)$$

Then quasi-reversible mixed relaxation processes (k_{e} = k_{d}) control water vapor diffusion over-potential (Tab. 5):

- from September end to November in the couple with the thermal energy - molar gas pressure:
  $F\eta_{\text{d}} = -p^{\theta} = -RT_{\text{w,v}} = -2{,}1$ kJ/mol
- in December in the couple with depolarized hydrogen over-potential on iron:
  $F\eta_{\text{d}} = -\eta(H_2/Fe) = -\Delta G^{\theta}_{\text{cor}} = -7{,}61$ kJ/mol due to the couple with indirect reaction on the side of gas phase:
  $E^{\theta}(O_2+H_2O+2e=OH^-+HO_2^-) = 7{,}3$ kJ/mol.

From September to December overall kinetic of atmospheric corrosion slowest velocity control the successive hydrogen depolarization titration. These processes were applied previously in gaseous arsenic hydride generation and successive cadmium and lead traces deposition on metal cathode of galvanostatic generated corrosion cell [17].

4 Conclusion

Recorded data from sun photometer and weather station were used in the monitoring of water vapor pressure in the atmosphere. The investigation results of the seasonal water vapor atmospheric corrosion kinetic, based on the fundamental chemical and electrochemical thermodynamics conservation law indicate to:

- Hydrogen corrosion type couple standard potential of indicator of stationary polarization of corrosion cell, from March to May,
- Water vapor diffusion over potential couple thermal collisions energy or oxygen chemical reaction from September to December.

The obtained results indicate that the difference between saturated water vapor pressure and measured values on the basis of sun photometer data affects considerably the atmospheric corrosion seasonal kinetic, controlled with the evolved hydrogen polarization (from March to August) and adsorbed hydrogen depolarization processes (from September to December).

The known seasonal mechanism would make possible to choose optimized corrosion protection methods, air purifying technological methods, catalytic metals deposition depending on atmospheric corrosion seasonal kinetic and other measures of protection against this major destroying phenomenon.

Acknowledgement

The paper is based on the project AirQ - Novel tool for urban air quality monitoring, with Project Code: 93/03.01.2012/ 5 Ro-Fr 2012. The work was partially supported by the strategic grant POSDRU/89/1.5/S/57649, Project ID 57649 (PERFORM-ERA), co-financed by the European Social Fund/Investing in People, within the Sartorial Operational Program for Human Resources Development 2007 ÷ 2013.

5 References

[1] Kaufman, Y. J.; Tanré, D.; Boucher, O. A Satellite View of Aerosols in the Climate System. // Nature. 419, (2002), pp. 215-223.

[2] Dubovik, O.; Holben, B.; Eck, T. F.; Smirnov, A.; Kaufman, Y. J.; King, M. D.; Tanre, D.; Slutsker, I. Variability of Absorption and Optical Properties of Key Aerosol Types Observed in Worldwide Locations. // Journal of the Atmospheric Sciences. 59, (2002), pp. 590-608.

[3] Dubovik, O.; Smirnov, A.; Holben, B.; King, M. D.; Kaufman, Y. J.; Eck, T. F.; Slutsker, I. Accuracy Assessments of Aerosol Optical Properties Retrieved from AERONET sun and sky radiometric measurements. // Journal of Geophysical Research. 105, (2000), pp. 9791-9806.

[4] Holben, B. N. et al. A Federated Instrument Network and Data Archive for Aerosol Characterization. // Remote Sensing of Environment. 66, (1998), pp. 1 – 16.

[5] Popescu, F.; Ionel, I.; Talianu, C. Evaluation of Air Quality in Airport Areas by Numerical Smulation. // Environmental Engineering and Management Journal. 10, 1(2011), pp. 115-120.

[6] Popescu, F.; Ionel, I.; Lontis, N.; Calin, L.; Dungan, I. L. Air Quality Monitoring in an Urban Agglomeration.// Romanian Journal of Physics. 56, 3, 4 (2011), pp. 495-506.

[7] Ionel, I.; Nicolae, D.; Popescu, F.; Talianu, C.; Belegante, L.; Apostol, G. Measuring Air Pollutants in an International Romania Airport with Point and Open Path Instruments. // Romanian Journal of Physics. 56, 3,4(2011), pp. 507-519.

[8] Vetres, I.; Ionel, I.; Popescu, F.; Lontis, N. Air Pollution Analysis in Western Romania and the Necessity of Complementary Vertical Resolved LIDAR observation. // Optoelectronics and Advanced Materials – Rapid Communications. 4, 8(2010), pp. 1256-1260.

[9] International Standard 9845-1 Solar energy – Reference Solar Spectral Irradiance at the Ground at Different Receiving Conditions, Geneva. http://ncar.ucar.edu/.// International Organization for Standardization, ISO, 1998.

[10] Calinoiu, D.; Trif-Tordai, G.; Ioana, I.; Pavlović, M.; Popescu, F.; Ševaljević, M.; Makra, L.; Lontis, N. Study on Atmospheric Water Vapor Content, Comparing Data Collected from Weather Station, and Sun Photometer Direct Measurements. // Ecology of Urban Areas, Proceedins of the 2nd International Conference / Zrenjanin, 2012, pp. 13-18.

[11] Calinoiu, D. Research Regarding the Influence of Aerosols upon Solar Energy Potential by Applying the Atmospheric Radiative Transfer, PhD Thesis, Politehnica University of Timisoara, 2012.

[12] Tschamler, H. E.; DeRuiter, Trassatti, S. In Chemistry of Coal Utilization, Ed. Part B. Elsevier, New York, 1981.

[13] Šušić, M.; Minić, D.; Marinković, S. Electrochemical Gasification of Coal. // J. Serb. Chem. Soc. 57, 10(1992), pp. 705-713.

[14] Ševaljević, M. M.; Simić, S. N.; Ševaljević, P. V. Thermodynamic Diagnostic of Electron Densities in Gas Bubbles in Aerated Saturated Refinery Waste Water. // Desal. Wat. Treat. 42, (2012), pp. 144-154.

[15] Bard, A. J.; Parsons, R.; France, M.; Jordan, J. IUPAC Standard Potentials in Aqueous Solutions, Eddited by Marcel Dekker Inc., New Jork, Basel, 1983.

[16] Ševaljević, M. M.; Stanojević, M. M.; Simić, S.; Ševaljević, V. M. Water Entropy Driven Relaxation of Dissolved Oxygen in Refinery Waste Water. // Desalination and Water Treatment, doi: 10.1080/19443994.2013.800251 (21.04.2013)

[17] Ševaljevic, M. M. The Development of the Galvanostatic Method for Gaseous Arsenic Hydride Generation and Successive Lead and Cadmium Deposition for Increasing AAS Determination Sensitivity, Ph D Thesis, Faculty of Technology, Novi Sad, 2000.

Authors' addresses

Ševaljević Mirjana, Ph.D. corresponding author
- *associated professor* Technical Faculty "Mihajlo Pupin" in Zrenjanin of University in Novi Sad
- *professor of applied science*
in Technical College of Applied Science in Zrenjanin
Ul. Đorđa Stratimirovića 23, 23 000 Zrenjanin
Tel.: +00 381 23 565 896, Fax: +00 381 23 565 896
Mobil: + 00 381 61 3240207
E-mail: sevaljevic.mirjana@gmail.com

Delia-Gabriela Calinou, Assist. Dr. ing.
Universitatea Politehnica Timisoara
Bv. Mihai Viteazu, No 1, 300222 Timisoara, Romania
Tel.: +4.0256.403746
Mobil: +4.0749.232443
E-mail: delia.calinoiu@yahoo.com

Ioana Ionel, Prof. Dr. ing. habil
Universitatea Politehnica Timisoara
Bv. Mihai Viteazu, No 1, 300222 Timisoara, Romania
E-mail: ioana.ionel@mec.upt.ro

Milan Pavlović, Prof. Dr.
Technical Faculty "Mihajlo Pupin" in Zrenjanin of University in Novi Sad
Đure Đakovića bb, 23000 Zrenjanin, Serbia

Laszlo Makra, PhD
University of Szeged
6720 Szeged, Dugonics tér 13, Hungary

Ion Vetres, PhD
Universitatea Politehnica Timisoara
Bv. Mihai Viteazu, No 1, 300222 Timisoara, Romania

Gavrila Trif-Tordai, PhD
Universitatea Politehnica Timisoara
Bv. Mihai Viteazu, No 1, 300222 Timisoara, Romania